Geomicrobiology Journal, 19:485–504, 2002
Copyright © 2002 Taylor & Francis
0149-0451/02 $12.00 + .00
DOI: 10.1080/01490450290098450

Determination of Manganese Stability in a Constructed Wetland Sediment Using Redox Gel Probes

H. M. EDENBORN
L. A. BRICKETT

U.S. Department of Energy
National Energy Technology Laboratory
Pittsburgh, Pennsylvania, USA

Redox gel probes containing immobilized particulate manganese compounds (MnO_2, $MnCO_3$, and MnS) were placed on a surveyed grid in the sediment of a wetland receiving coal mine drainage in western Pennsylvania (USA). The stability of these compounds in the wetland was shown to be highly variable both temporally and spatially, indicating that apparent manganese removal based on water quality data did not result in long-term manganese retention in sediments. Contour maps of the gel probe data revealed the importance of local environmental conditions, such as surface water velocity, on geochemical conditions influencing manganese compound stability in sediments, as well as seasonal changes in the ability of the wetland to retain MnO_2 in sediments. Estimates of in situ MnO_2 reduction rates using gel probe data agree with earlier published estimates based on laboratory studies. Although the factors influencing particulate metal stability in sediments are extremely complex and difficult to study, the redox gel probe method is demonstrated to be a cost-effective means of obtaining an areal and depth-related picture of that stability during a particular period of time.

Keywords alabandite, coal mine drainage, early diagenesis, iron monosulfide, manganese, manganese oxide, redox gel probes, rhodochrosite, sediments, wetlands

Introduction

Coal mine drainage is a common water pollution problem on active and abandoned mine sites in the eastern United States. These waters often contain ferrous iron, ferric iron, aluminum, calcium, sodium, potassium, magnesium, manganese, and sulfate as their primary ionic components, and typically range in pH from ca. 1 to 8 (Hyman and Watzlaf 1997). In recent years, constructed wetlands have been used by mining companies and others to attempt to treat these waters, with the goal often being to meet regulatory discharge requirements by lowering total metal concentrations and acidity via natural physical, chemical, and biological reactions. The effective removal of iron and manganese from mine drainage by selected wetland systems has led to analyses of the factors contributing to their treatment successes

Received 6 October 2000; accepted 22 August 2001.
We thank the wetland property owners for ready access to the study site. Dr. Robert Thompson of Parsons Power Services, Inc., provided ICP-OES chemical analyses, and Elizabeth Frommell provided XPS analytical services. Our thanks to Debbie Burse and Darryl Dvorak for excellent technical assistance in the laboratory and field, respectively.
Address correspondence to: Harry M. Edenborn, U.S. DOE, National Energy Technology Lab, Mail Stop 83-226, P.O. Box 10940, Pittsburgh, PA 15236-0940, USA. E-mail: edenborn@netl.doe.gov

(Flanagan et al. 1994; Stark and Williams 1995), and geochemical investigations related to the redox-cycling of metals in the wetland sediments (Tarutis and Unz 1990, 1995; Tarutis et al. 1992; Stark et al. 1995). Although valuable conclusions regarding the probable stability and mobility of redox-sensitive elements have been made, a common problem facing all of these sediment studies is the apparent wide spatial variability seen in solid phase and porewater data collected from site to site within a given wetland. Hunt et al. (1997) noted wide variations in the geochemical profiles of constructed and natural wetland sediments sampled on a 0.15-m scale, and noted that more information is to be gained in geochemical studies of wetlands by placing emphasis on spatial, rather than temporal, sampling. Researchers face an understandable dilemma in deciding how to sample such complex environments and ration available time and resources to these activities in an effective manner.

A great deal of information about the geochemical cycling of Fe and Mn in a wetland can be obtained from sedimentary solid phase and porewater chemical profiles (Berner 1980). However, the processing of sediment cores can be time-consuming and expensive, especially if numerous cores must be taken to characterize a given area. Interstitial water samplers ("peepers") based on the diffusion of solutes across membranes into sampling chambers often cannot provide the appropriate fine-scale vertical resolution necessary to observe transitions in the distribution of redox-sensitive elements (Brandl and Hanselmann 1991). In another article in this issue (Edenborn et al. 2002), we introduced the concept of the redox gel probe, a simple device used to assess the degree of stability of redox-sensitive trace elements in shallow wetland sediments. The redox gel probe consists of a grooved plastic rod containing an agar gel immobilizing a homogenous suspension of a particulate compound of geochemical interest. The probes are inserted vertically into sediments and are left in place for a period of time, after which they are recovered and analyzed, either visually, chemically, or both. Preliminary field work with MnO_2-containing gel probes in a constructed wetland demonstrated that gel-immobilized MnO_2 underwent various chemical transformations while in situ, ranging from partial to complete solubilization of the particles, to the apparent coating or replacement of the MnO_2 by iron oxides and gypsum. In the current study, we examined the response of redox gel probes containing four different redox sensitive compounds of geochemical interest within a study wetland receiving mine drainage from an abandoned underground coal mine and associated waste piles.

Materials and Methods

Field Studies

Study site. Field studies were conducted in a constructed wetland located near the town of Sligo, in northwestern Pennsylvania (41°08′29″N, 79°29′21″W). The wetland area (Figure 1) was created in 1986 by a coal mining company by pooling water behind hay bale and earthen dams, and flooding an organic substrate mixture of spent mushroom compost, mulched hay, and agricultural lime. The wetland was built to facilitate manganese removal from the mine drainage by algae, which formed thick floating mats in the standing water during the summer. The specific study location consisted of a relatively open water area immediately upstream from a discrete outlet that drained all water collected by the wetland complex (Figure 1). The area was mapped and a 5 × 6-m study grid was established using a tape measure and optical transit. Water entered the study area via a channel that led from an abandoned underground coal mine 0.7 km upstream of the wetland, as well as from numerous small springs and seeps draining adjacent mine spoils. The predominant vegetation in the wetland was the broad-leaf cattail, *Typha latifolia* L., although the open

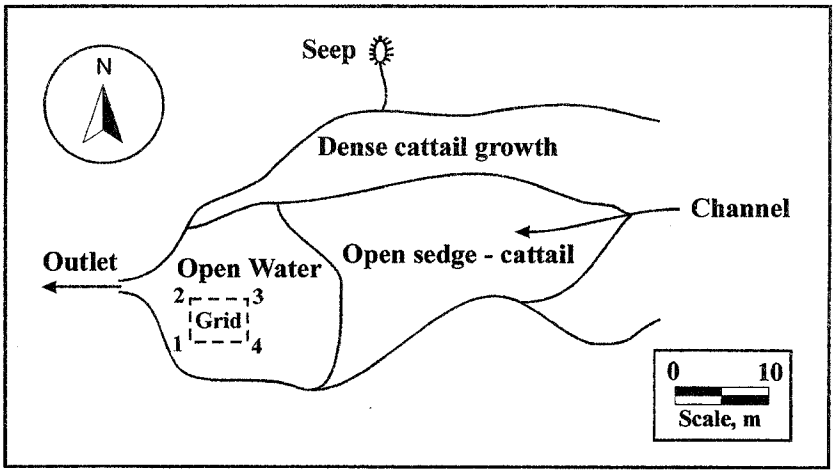

FIGURE 1 Site map of the wetland study area. The study area is approximately 0.7 km downstream of the deep mine discharge located to the extreme right of the map. The locations of the 5 × 6-m study grid with sampling locations 1 through 4, a perennial acid seep, and the principal channel of drainage from the deep mine discussed in the text are shown.

water area principally contained a mixture of grasses and sedges. The wetland open water area developed extensive floating algal mats in the early summer (ca. June), which sank to the sediment surface later in the summer (ca. August). Almost 90% of the 360 hectare watershed surrounding the wetland site had been impacted by surface and underground coal mining during the previous 50-year period (C & K Coal Company 1986).

Sample collection. Surface water samples were collected at the various inlets and the outlet of the study wetland. High-density polyethylene sample bottles were cleaned by acid washing and rinsing with deionized water. Random bottles were selected for blank analysis. Then 200-ml samples for metals analysis were passed through 0.45-μm membrane filters (SFCA membrane; Corning, Inc., Corning, NY, USA) and were acidified with 2 ml trace metal-grade concentrated HCl to pH < 2. Apparent changes in the chemical composition of the mine drainage as it flowed through the study area were assessed on two occasions (high and low flow) by comparing water quality in the effluent channel with the flow-weighted average quality of water coming from the influent channel and small seeps. Flow volume estimates were made using a bucket and stopwatch for small seeps and the velocity-area method (Wahl et al. 1995) for larger channels.

Interstitial porewater samples were collected using equilibrators similar to those designed by Hesslein (1976). The specific method used is described in detail in Edenborn et al. (2002). The geochemical assessment model MINTEQA2/PRODEFA2 (Version 3.0; Allison et al. 1991) was used to determine the saturation state of solid carbonate mineral phases based on the chemical composition of the porewater samples.

Sediment cores were collected by manually inserting 5.5-cm inner diameter Plexiglas core tubes into the sediment. Rubber stoppers were placed in the bottoms of the core tubes by hand prior to their removal from the sediment. A simple piston was used to extrude the sediment core upward after the surface water had been siphoned off, and 1-cm core sections were collected as the sediment was exposed. The outside layer of each section was removed to eliminate contamination due to core smearing. Sediment sections were then placed in clean water sample bottles and frozen on dry ice prior to further analysis. Data were not corrected for the possible influence of core shortening (Morton and White 1997).

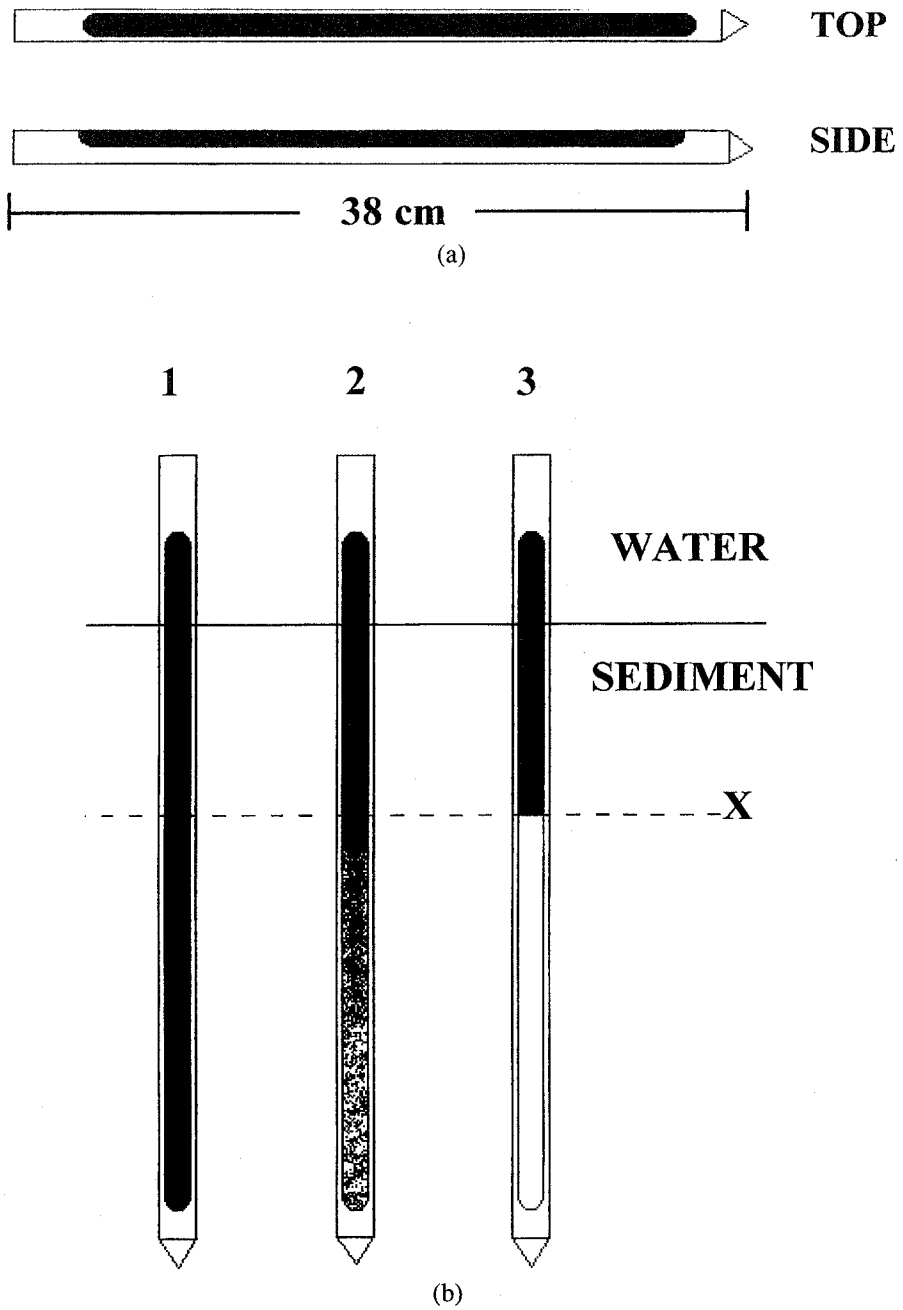

FIGURE 2 (a) Schematic of the redox gel probe containing 2% (wt/vol) agar with immobilized MnO_2 particles. (b) Method of redox gel probe placement in the sediment. X represents the variable and hypothetical sediment depth below which particle dissolution begins to occur due to reaction with diffusable reductants. The general appearance of MnO_2-containing gel probes: 1) upon initial insertion; 2) after intermediate incubation (partial particle dissolution); and 3) after maximum incubation (complete dissolution). Although complete gel clarification can occur as shown in (3), dissolution of immobilized redox-sensitive precipitates may also be accompanied by the formation of other secondary solid compounds.

Analytical methods. Field measurements of pH were made using an Orion SA270 portable field meter and a combination pH electrode using a two-point calibration. Redox potential was determined with an epoxy-body redox platinum combination electrode. Alkalinity (as $CaCO_3$ equivalents) was determined by titrating samples with 0.2 N H_2SO_4 to pH 4.8 (U.S. EPA method 310.1). Acidity was also measured titrimetrically (U.S. EPA method 305.1). Sulfate concentrations were analyzed by barium chloride titration, using thorin as the endpoint indicator, following passage of the raw sample through a cation exchange column. All other ions were determined by Inductively Coupled Plasma Optical Emission Spectroscopy (ICP-OES) on a Perkin Elmer Optima 3000 Radial-View spectrometer. The sensitivities were $\pm 2\%$ and the detection limits were ≥ 0.05 mg/L for all metals. The U.S. Environmental Protection Agency quality control guideline of one duplicate, one standard recovery, and one spike recovery for every 10 analyses was employed (U.S. EPA 1983). Sediment samples for total metals analysis were oven-dried to a constant weight at 105° C and were digested in a 1:1 (vol/vol) mixture of concentrated HCl and concentrated HNO_3 prior to analysis by ICP-OES.

Redox gel probe construction. Probes were constructed as described previously (Edenborn et al. 2002). Briefly, metal compound precipitates were prepared (see later) and homogeneously suspended in solutions of purified 2% (wt/vol) Bacto agar (Fisher Scientific Co., Pittsburgh, PA, USA) dissolved in boiling deionized water. An 8-ml aliquot of each suspension was transferred by pipette to the longitudinal groove in a specially prepared gel holder (Figure 2a) on a level surface and was allowed to cool. After the agar had solidified (usually within 1 min), the gel probes were stored under inert gas in plastic bags and were used in the field within 4 h. In specific experiments, control gels were removed from their holders immediately following solidification or after incubation in the field. These gels were sliced into 1-cm sections with a clean razor blade, digested in a 1:1 (vol/vol) mixture of concentrated HCl and HNO_3, brought to constant volume, and analyzed for total metals by ICP-OES.

Gel probe precipitates. Four different precipitates were prepared in the laboratory and were used as model compounds in the current study: manganese dioxide, manganese carbonate, manganous sulfide, and iron monosulfide. X-ray diffraction (XRD) analyses of the final precipitates were done using a Rigaku Geigerflex powder diffractometer (Rigaku/MSC, The Woodlands, TX, USA) and Jade 3.1 software (Material Data Inc., Livermore, CA, USA).

Manganese dioxide precipitate was prepared by adding 500 ml of 20 mM $KMnO_4$ (adjusted to pH 12.4 with 1N NaOH) drop-wise to a vigorously stirred solution of 1 L of 20 mM $MnSO_4 \cdot H_2O$. The resulting fine brown/black precipitate was mixed for an additional 15 min and allowed to settle. After 15 min, the supernatant was decanted, and the precipitate was washed with five 1.5-L volumes of deionized water in a similar fashion. Dissolved manganese concentrations in the final wash water were low (between 2–19 mg/L) and the final pH was between 6 and 7. The precipitate was stored in the final wash water prior to use. XRD analysis indicated that this precipitate preparation was initially amorphous, but became more crystalline within a few days, giving variable but detectable XRD refraction patterns consistent with the manganese oxides akhtenskite (ε-MnO_2, hexagonal), ramsdellite (MnO_2, orthorhombic), hausmannite (Mn_3O_4, tetragonal), and birnessite ($Na_2Mn_{14}O_{27} \cdot 9H_2O$, monoclinic).

Manganese carbonate was prepared by adding an aqueous solution of 1 M Na_2CO_3 to a continuously stirred 1 M $MnCl_2$ solution until the pH rose to approximately 7. This was done to avoid the formation of $Mn(OH)_2$ at a higher pH. Both solutions were deoxygenated with argon gas prior to use. The resulting pink precipitate was washed with and stored in high-purity deionized water purged with argon gas. XRD analyses of samples preserved under

petroleum jelly indicated that the only crystalline compound present was rhodochrosite ($MnCO_3$).

Manganous sulfide was prepared by heating 100 ml of a 2 M $Na_2S \cdot 9H_2O$ aqueous solution to boiling in a 500-ml flask fitted with a reflux tower (Weiser and Milligan 1931). A 25-ml solution of 1 M $MnCl_2 \cdot 4H_2O$ was added slowly to the boiling solution. A pink floc formed immediately, which gradually (20–30 s) became green. The solution was heated for an additional 5 min. After the solution had cooled, the precipitate was washed and stored in high-purity deionized water purged with argon gas. The precipitate was washed with 100 ml deoxygenated deionized water each day for 3 days. Exposure of the lime-green precipitate to air resulted in a rapid color change to a brown-black color; in MnS-containing gel probes, a slight precipitate color change had usually begun at the gel-air interface at the time of probe insertion into the sediment. XRD analysis of samples preserved under petroleum jelly indicated that the green precipitate was alabandite (MnS), containing occasional trace amounts of pyrochroite [Mn $(OH)_2$] when some sample oxidation occurred prior to analysis.

Iron monosulfide precipitate was prepared by adding 1 ml of a 2.4 M aqueous solution of $Na_2S \cdot 9H_2O$ to 250 ml of a 28-mM aqueous solution of $FeSO_4 \cdot 7H_2O$. The supernatant was decanted, and the black precipitate was washed 5 times with 250 ml deoxygenated deionized water. XRD analysis of this precipitate preserved under petroleum jelly indicated an amorphous crystal structure.

Field deployment of redox gel probes. Probes were placed in the sediment along established transects or grids. Sediment/substrate thickness at each sample point was initially measured when the study grid was first surveyed. Substrate thickness was defined as the depth below the sediment-water interface that could be manually penetrated using a calibrated 2.5-cm diameter PVC pipe (Stark and Williams 1995). Each probe was placed vertically into the sediment so that approximately 4 cm of the agar gel remained above the sediment-water interface (Figure 2b). The height of the gel probe initially extending above the sediment surface was noted as a check on any further sediment deposition during the incubation period.

Grid studies. Redox gel probes containing particulate MnO_2, $MnCO_3$, MnS, and FeS, respectively, were placed in the sediment of the wetland at 1 m intervals on a 5 × 6-m surveyed grid (30 m^2; 42 total sample points; Figure 1) in September. Four probes were placed in the sediment at each sample point as a single gel "cluster," or group of four held together at top and bottom with rubber bands and configured so the exposed gel in each probe faced outward. Although the slow rate of water flow during the sampling period did not appear to affect individual probes within these clusters differently, the orientation of the gels relative to water flow in a given system may need to be considered. On a second occasion (the following June), MnO_2 gel probes only were placed on the same grid points, left in place for 9 days, analyzed, and plotted as described later. Care was taken to avoid disturbance of the sediment within the sample grid. Access to grid sample points that could not be reached by hand from the outer boundaries of the grid was accomplished by floating on an inflatable rubber raft. After 9 days of incubation, the probes were removed and the visible zones of precipitate stability or transformation were measured relative to the location of the sediment-water interface. Each probe type used in this study exhibited a depth where a sharp contrast in color change was observed, marking the oxidation, reduction, or disappearance of the initially immobilized precipitate. MnO_2 underwent a change from a dark brown/black gel to a clear or white-colored gel upon reduction and solubilization at depth. $MnCO_3$, MnS, and FeS remained their initial colors (white, green, and black, respectively) at depth in the sediment, but changed to a clear, gray, or orange color closer to

the surface. Selected sections of the gels were excised and digested with acid for total metal analysis by ICP-OES. Compound stability depths (i.e., depth below the sediment-water interface to which MnO_2 remained stable/black, and depths below the interface at which the remaining reduced compounds remained stable) were plotted as contour maps using the Kriging gridding method (Surfer for Windows, version 6; Golden Software, Inc., Golden, CO, USA). The barely discernable water current flow rate within the grid was calculated after repeated measurements of the distance traveled by neutral buoyancy particles timed with a stopwatch.

Results

Water Quality

Table 1 shows the range in water quality in the study wetland effluent as determined on random sampling dates over a 4-year period. The wetland effluent was typically a neutral to slightly acidic pH water that was sulfate-rich, moderately elevated in dissolved manganese, and relatively free of dissolved iron. Almost all of the ca. 30 mg/L total iron initially present in drainage leaving the underground mine 0.7 km upstream was removed from solution prior to reaching the study site (data not shown), but small seeps from surrounding spoil piles also supplied erratic inputs of dissolved iron. Additional soluble metals detected on occasion in the wetland effluent included Co (0.2–0.6 mg/L), Ni (0.2–0.8 mg/L), Zn (0.2–0.4 mg/L), and Cu (1.1 mg/L). A comparison of these data with a survey of 128 different coal mine drainages from 10 U.S. states (Hyman and Watzlaf 1997) indicates that the study wetland water is high in pH, alkalinity, calcium, magnesium, and potassium, and low in sulfate and iron, relative to most regional coal mine drainage. Manganese concentrations reported in the survey averaged ca. 22 mg/L (ranging from 0 to 164 mg/L; Hyman and Watzlaf 1997), compared to the 15.2 mg/L average for the study wetland.

The water quality of the effluent at the study site on any particular sample date was a complex function of the mixing of several different sources of water of differing composition. These sources consisted of the channel of water originating from the underground mine, a major seep draining acid-generating coal mine waste and overburden, and numerous intermittent seeps draining alkaline mine wastes. Tables 2a and 2b show estimates of the daily loads of the major aqueous ions entering and exiting the study area during periods of low and high rainfall within the watershed during the month of June on two successive

TABLE 1 Effluent water quality[a] for study wetland measured over 4 years (n = 23)

Parameter	x ± SD	Minimum	Maximum
Alkalinity (as $CaCO_3$)	37.3 ± 65.7	−57	140
Calcium	380 ± 33	275	434
Iron (total)	0.68 ± 0.28	<0.1	1.3
Magnesium	253 ± 37	191	309
Manganese	15.2 ± 3.8	5	23
Potassium	9.6 ± 1.1	7.7	10.9
Sodium	15.4 ± 2.6	11.5	18.5
Sulfate	1872 ± 123	1470	2061
pH	6.45 ± 0.6	5.05	7.8

[a]Measured in units of mg/L, except for pH. Average alkalinity was calculated using both the measured acidity and the measured alkalinity. Acidity was considered to be negative alkalinity.

TABLE 2a Daily loads of the major aqueous ions entering and exiting the wetland study area during a period of low flow

	Acidic seep	Alkaline seeps	Wetland channels	Combined influent	Combined effluent	Percent removed[a]
			Aqueous ion load, moles/d			
Alkalinity	−46	614	18	586	287	51
Calcium	445	1483	73	2001	1949	3
Magnesium	578	1554	77	2209	2134	3
Manganese	41	61	2	104	48	54
Potassium	11	36	2	49	41	16
Sodium	33	97	4	134	132	1
Sulfate	1088	2791	144	4023	3985	1
			Flow, m^3/d			
	46	135	8	189	189	

[a] Flow calculated for wetland channels was adjusted to balance study area estimated influent volume with measured effluent volume. Removal calculations do not account for potential ion influx from the sediment.

years. The total effluent volume during the period of high flow was 6 times that observed during the low flow period, and thus represents a much shorter residence time for water within the wetland. The data suggest that total loads of alkalinity, Mn, and K were decreased on both dates during passage through the wetland.

Study Grid Characteristics

Figure 3 illustrates the spatial distribution of several physical characteristics of the 30-m^2 study grid at the time of redox gel probe placement. A slow (3 cm/sec) flow of water crossed the grid diagonally towards the wetland outlet (arrow; Figure 3a). The plotted contour maps show that this primary flow path resulted in a minor channel with a greater

TABLE 2b Daily loads of the major aqueous ions entering and exiting the wetland study area during a period of high flow

	Acidic seep	Alkaline seeps	Wetland channels	Combined influent	Combined effluent	Percent removed[a]
			Aqueous ion load, moles/d			
Alkalinity	−146	825	862	1541	658	57
Calcium	1,567	3,144	7,019	11,730	11,343	3
Magnesium	1,914	3,353	7,333	12,600	12,403	2
Manganese	120	140	211	471	387	18
Potassium	45	80	188	313	294	6
Sodium	108	207	428	743	743	0
Sulfate	3,720	6,301	14,358	24,379	24,251	1
			Flow, m^3/d			
	174	298	759	1,231	1,231	

[a] Flow calculated for wetland channels was adjusted to balance study area estimated influent volume with measured effluent volume. Removal calculations do not account for potential ion influx from the sediment.

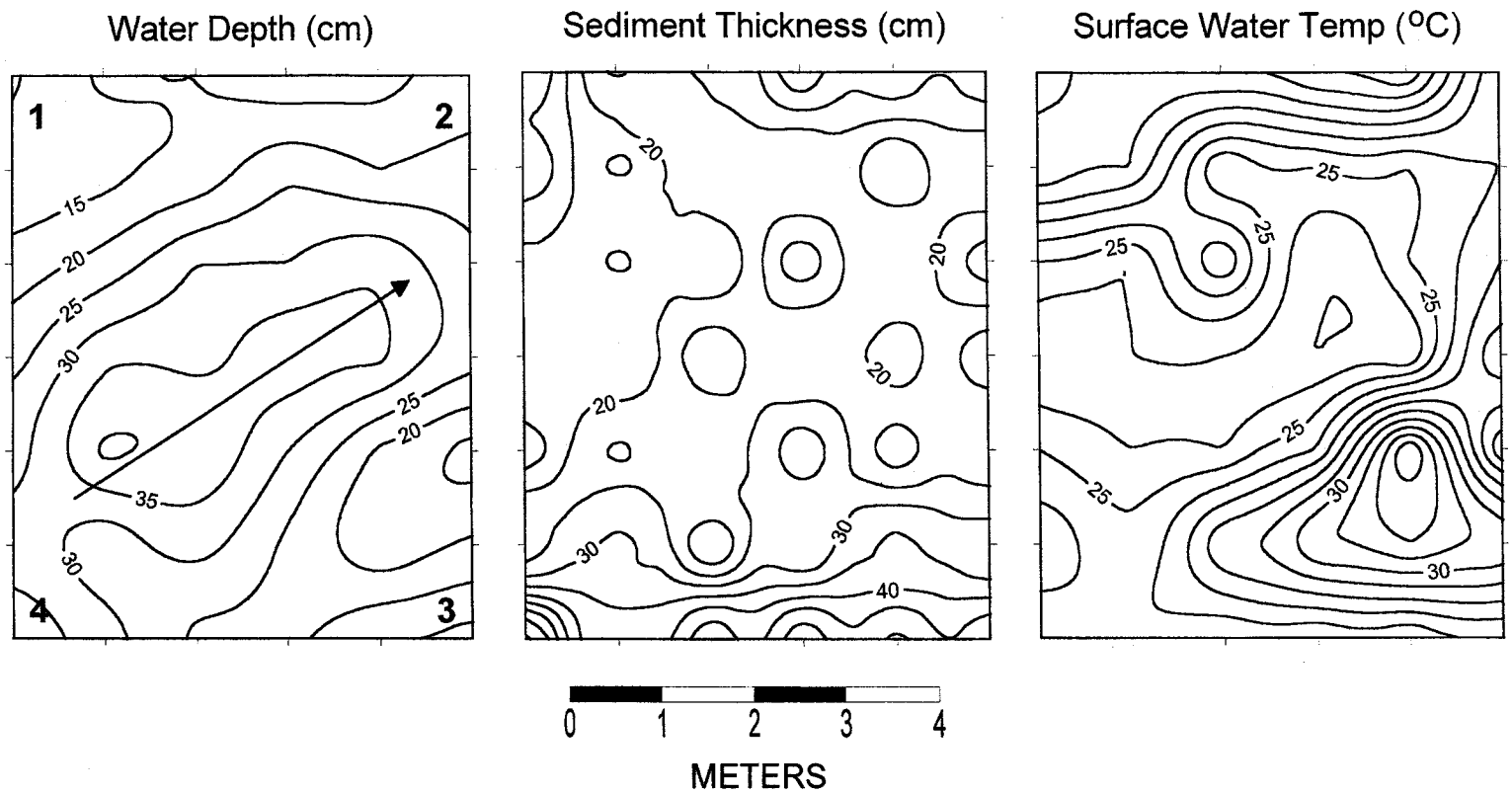

FIGURE 3 Contour maps showing the relative variation in a) water depth, b) sediment thickness, and c) surface water temperature in the 5 × 6-m wetland grid area in September. The arrow in Figure 3a indicates the general direction of the low rate of water flow (3 cm/sec) through the grid area. Numbers shown in the corners of the Figure 3a map indicate the orientation of the mapped region within the wetland study area (Figure 1).

depth of surface water and shallower sediment thickness (Figure 3a and 3b, respectively) than the surrounding area, probably due to periodic scouring of the flow path during high flow. This flow path also had a lower surface water temperature (Figure 3c). Temperature anomalies on the plotted map were usually due to the presence of floating algal mats, which tended to trap heat from solar radiation. Sediment depth (that readily penetrated with a PVC pipe) gives some measure of the present distribution of organic material initially placed in the wetland and any subsequent patterns of sediment deposition.

Sediment Porewater

Figure 4 shows the depth distributions of alkalinity, sulfate, redox potential, and manganese, respectively, in porewater collected in three equilibrator samplers placed in the study wetland in September. Sample locations correspond to the three corners (1, 2, and 3) of the surveyed grid that was established (Figure 1). In general, the observed profiles were similar in that they all exhibited increasing alkalinity with depth, decreasing redox potential with depth, subsurface maxima in dissolved manganese concentrations, and some degree of decrease in sulfate concentration with depth, suggestive of bacterial sulfate reduction activity. However, wide variations in the concentration profiles of these variables were observed between sample sites, suggesting that the diagenetic processes affecting metal stability were heterogeneous within the study wetland. Corner 1 of the grid was the shallowest, warmest, and had the most sluggish water flow, which may account for a greater degree of MnO_2 solubility (higher porewater dissolved Mn concentrations) and a more rapid decrease in sulfate concentration with depth. In contrast, the deepest location (#3) showed the slowest

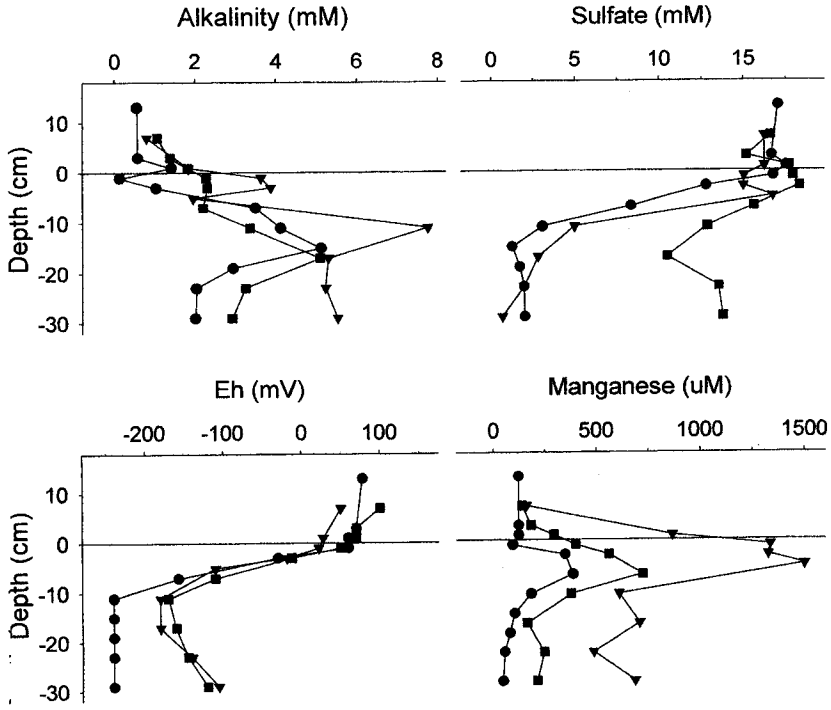

FIGURE 4 Porewater profiles of alkalinity, total dissolved sulfate, redox potential, and total dissolved manganese, corresponding to three different corners (1 = triangles, 2 = circles, and 3 = squares; Figure 1) of the wetland grid sampled on the same day in September.

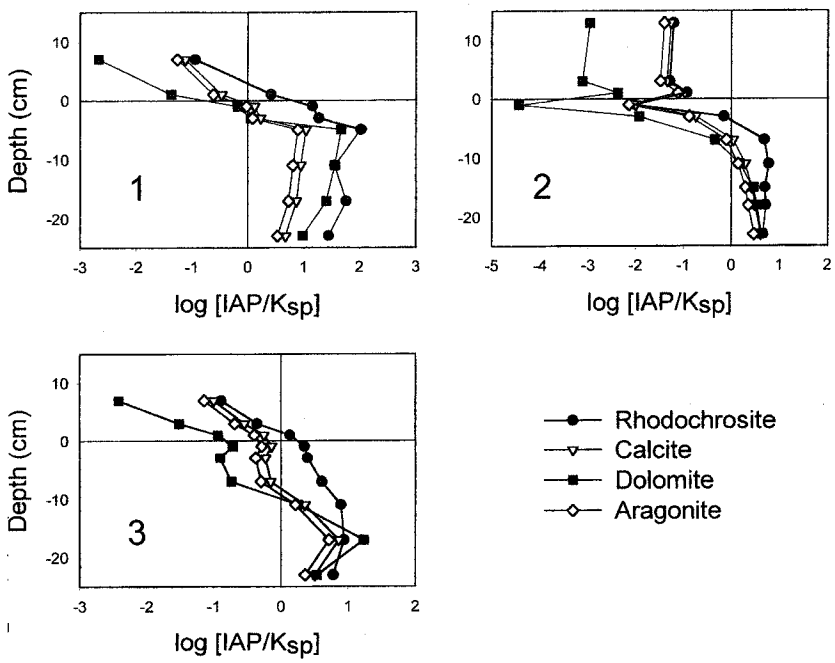

FIGURE 5 Saturation state of rhodochrosite, calcite, dolomite, and aragonite in the overlying water and with depth in the sediment at three locations in the study grid (corners 1, 2, and 3; Figure 1), corresponding to the samples shown in Figure 4. log [IAP/Ksp] >0 = supersaturated, <0 = undersaturated.

rate of decrease in sulfate concentration with depth, possibly due to the effect of cooler temperatures on bacterial sulfate reduction. Saturation index (Ω) values were calculated for four major carbonate minerals at the three locations ($\Omega = IAP/K_{sp}$, where IAP is the ionic activity product, and K_{sp} is the solubility product of pure mineral phase at 25°C; Figure 5). Given the inherent uncertainty in solubility calculations, these data suggest that the porewater becomes supersaturated with respect to all four mineral forms with depth in the sediment, with rhodochrosite ($MnCO_3$) being more likely to form prior to the other carbonate minerals. In addition, at sites 1 and 3, the data suggest that rhodochrosite may tend to form in the surface water and surficial sediments at this point in time.

Gel Probe Grid Analysis

Figure 6 shows the areal patterns of stability for gel probes containing particulate MnO_2, $MnCO_3$, MnS, and FeS, respectively, after 9 days of incubation in the study grid. Note that for MnO_2 probes, or those that contain an oxidized solid compound, greater stability is indicated by the increased depth below the surface to which the solid persists. In Figure 6a, MnO_2 remained stable to greater depths (ca. 2–4 cm subsurface) in the path of greatest water flow identified in Figure 3a. MnO_2 in probes was typically solubilized completely below the sediment surface in the corner #1 region of the grid. For the other three reduced compounds, greater stability is indicated on the maps by shallower depths of dissolution; i.e., the closer to the surface that these solid compounds persisted. Both $MnCO_3$ (Figure 6b) and FeS (Figure 6d) typically remained stable to within several cm of the sediment-water interface, suggesting that this stability may be largely linked to the depth of oxygen penetration into the sediment. Occasional anomalies were noted for all compounds, however, where the

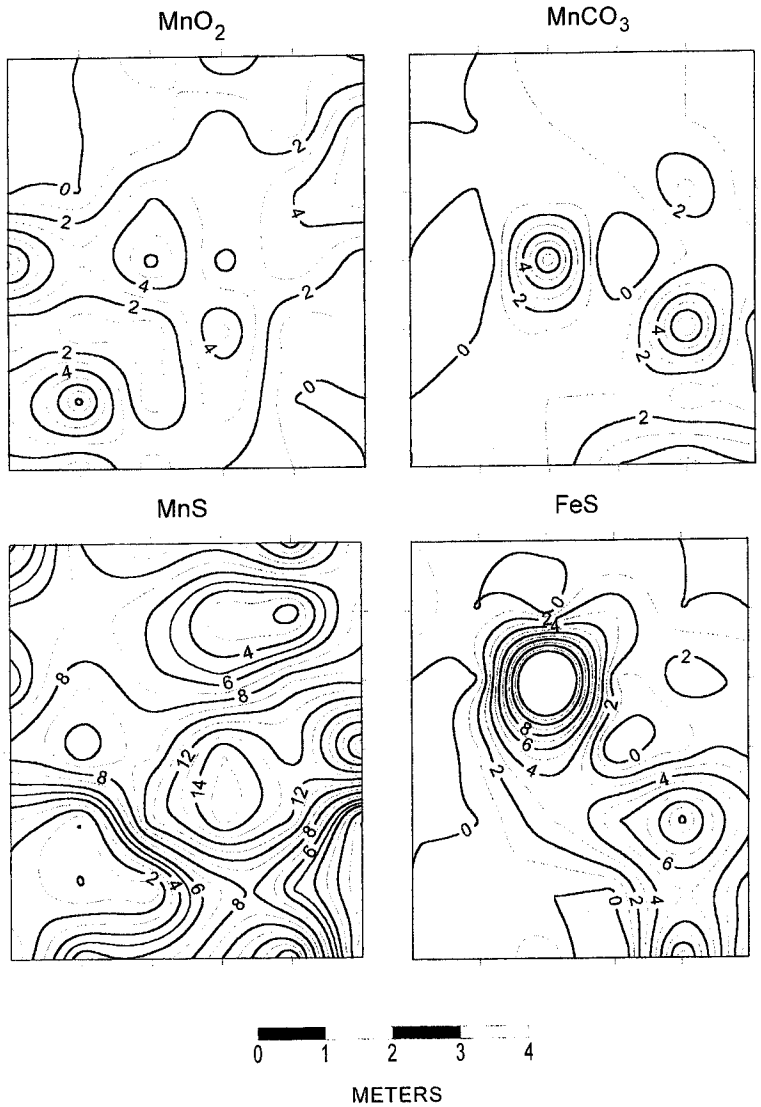

FIGURE 6 Contour maps showing the stability of MnO_2, $MnCO_3$, MnS, and FeS in redox gel probes placed in the wetland grid for 9 days during September. All depths are indicated in cm. MnO_2 stability is represented as the sediment depth to which solid MnO_2 persisted in the gel (i.e., MnO_2 was unstable below this depth). The stability of the other three reduced compounds is represented by the depth below which the compound was consistently persistent with depth (i.e., the compounds were unstable above this depth). Plots are shown in the same spatial orientation as described previously (e.g., Figure 3).

stability or instability of a given compound was widely different from surrounding grid points. Interestingly, MnS stability patterns (Figure 6c) appeared to be independent of the stability patterns of $MnCO_3$ and FeS, and be more directly and inversely correlated with the stability of MnO_2. In agreement with their relative solubilities, FeS was generally much more stable than MnS, which was only found in redox gel probes at greater depths in the sediment.

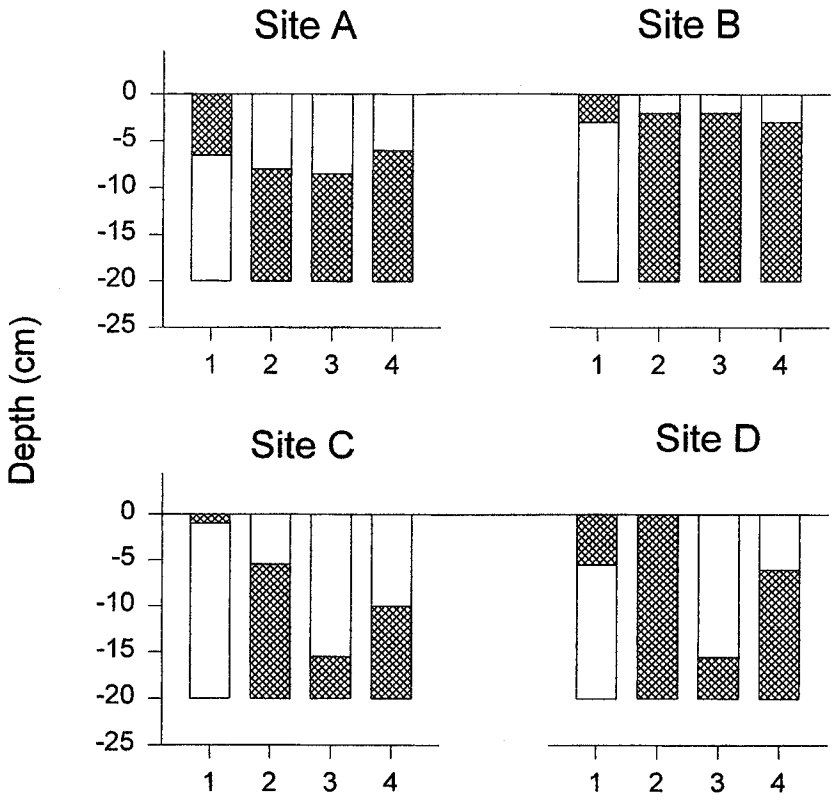

FIGURE 7 Regions of stability for particulate (1) MnO_2, (2) $MnCO_3$, (3) MnS, and (4) FeS in redox gel probes at four different sites in the study grid (Figure 6). Zones of particulate dissolution and stability in the gels are indicated by clear and cross-hatched sections, respectively.

The way in which stability of the four different compounds was interrelated at individual sites within the grid is shown in Figure 7. Both sites A and B show "classic" responses, where MnO_2 (#1) was stable in the uppermost sediments, and its reduction/solubilization at depth corresponded to an environment where the three reduced compounds were most stable. However, other scenarios were equally common. At site C, MnO_2 (#1) only remained stable just below the sediment-water interface, while $MnCO_3$ (#2) was not stable until several cm deeper in the sediment, and the two metal sulfides (#3 and #4) were not stable until much greater depths. Likewise, at site D, the pattern of stability was similar, but $MnCO_3$ was stable all the way to the sediment-water interface, despite the apparent stability of MnO_2 in the same shallow sediments as well. These data suggest that at some sites a common variable (such as oxygen concentration or sediment redox potential) may act on all four compounds to produce a predictable response, while at other sites, multiple variables result in less predictable patterns of compound stability.

Quantitative Analysis of Manganese Remaining in Gel Probes

Three MnO_2 probes were placed outside the study grid closer to the source of a seep that provides acidic and iron-rich water to the wetland on a periodic basis. An example of the quantitative analysis of total manganese remaining in each gel probe after incubation for 9 days is shown in Figure 8. A reduction of manganese content occurred at all depths in

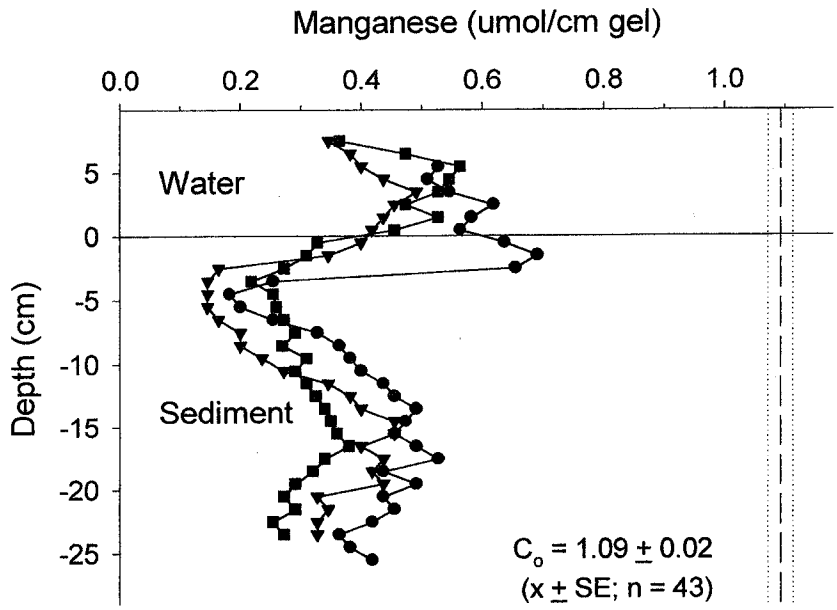

FIGURE 8 Concentrations of total manganese remaining in 3 gel probes after incubation for 9 days in sediments adjacent to the grid study. Vertical reference line shows the initial concentration of manganese per cm of gel probe (mean ± SE; n = 43).

the gel probe relative to the initial concentration added. The MnO_2 in these gels turned a distinct orange color at depth, with MnO_2 particles appearing to be coated with or replaced by iron oxides. The total iron content in the same three gels is shown in Figure 9. Although the greatest amount of initially added manganese was reduced in the sediment depth interval of ca. 2 to 7 cm below the sediment-water interface, the greatest accumulation of iron in MnO_2 gel probes occurred at somewhat greater depths.

Seasonal MnO_2 Stability

The study grid was analyzed with MnO_2 gel probes a second time 10 months after the first study to determine whether changes had occurred in the sediment that would influence net MnO_2 stability. The results (Figure 10) showed very apparent differences in gel probe MnO_2 stability during the two study periods. The September grid was characterized by very shallow depths of MnO_2 stability in the sediment, which accompanied warm water temperatures, and fresh and abundant organic matter from decaying algal mats. In contrast, in the early summer of the following year (June), MnO_2 was stable to much greater depths below the sediment-water interface under colder water conditions (ca. 10°C) and prior to the onset of algal mat formation. This type of comparison suggests that MnO_2 accumulation in these wetlands may be much more likely to occur during particular times of the year, and that manganese removed from solution and accumulated in the wetland sediment is likely to be remobilized in a gradual and spatially selective manner.

Discussion

The collection of three or more sediment samples from a freshwater wetland usually provides sufficient evidence of the remarkable heterogeneity and complexity of this environment.

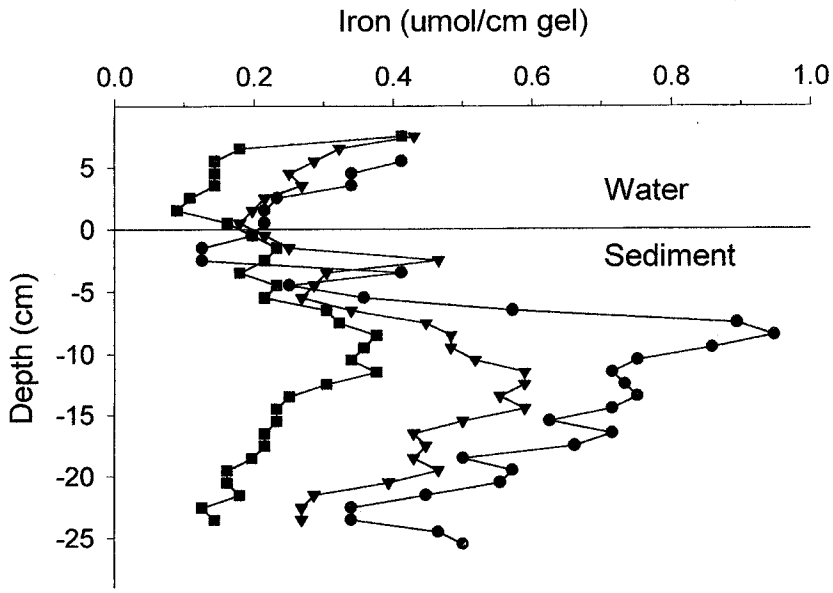

FIGURE 9 Concentrations of total iron in 3 MnO_2 gel probes (Figure 8) incubated for 9 days in sediments adjacent to the grid study.

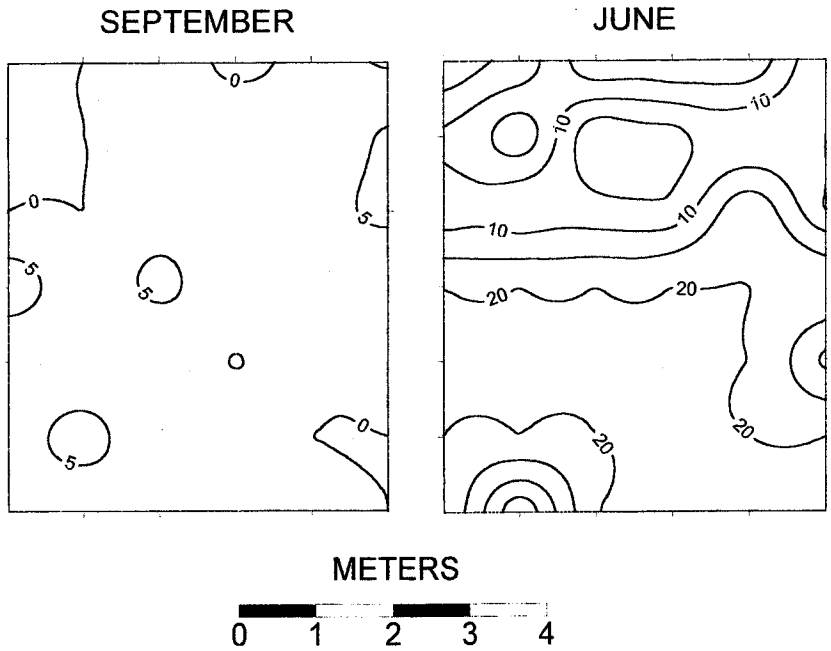

FIGURE 10 Contour maps showing the relative stability of MnO_2 in redox gel probes placed 10 months apart in the same wetland grid (n = 42 for each map; all depths are indicated in cm). MnO_2 stability is indicated as the depth to which solid MnO_2 persisted in the gel before visibly being partially or completely solubilized. In each case, gels were incubated in situ for 9 days.

Limited sampling time and resources result in the geochemical oversimplification of such systems and tend to result in the neglect of natural variability on a spatial basis (Hunt et al. 1997). In addition, the variables inducing change in the stability of a specific compound of interest may be numerous, and knowledge of their individual intensities or activities simply too complex to unravel. To address this problem, the redox gel probe approach is used to examine the net stability of particular solid compounds of geochemical interest, without addressing the specific mode of action of any particular agent of dissolution.

The redox gel probe approach affords an opportunity to carry out the simultaneous titration of a common initial substrate along continuous depth profiles within a specified study area. This approach is in contrast to many recent and innovative quantitative applications of gel probes developed for the extremely fine-scale resolution of dissolved metals in sediments. In these approaches, gels either establish equilibrium with metals in the porewater (e.g., Krom et al. 1994; Harper et al. 1997) or develop a defined diffusion gradient in films under conditions of controlled mass transport (e.g., Davison et al. 1997). Recent examination of the fine-scale distribution of dissolved iron and manganese in sediment porewaters of a seasonally anoxic lake using a gel diffusion approach showed extreme heterogeneity in the spatial distribution of these metals, which differed greatly in samples only 3 mm apart (Shuttleworth et al. 1999). These authors suggested that microniches are likely to play a dominant role in metal solubilization in sediments.

The patterns of manganese compound stability observed in the wetland investigated in this study are in agreement with other observations for similar wetlands in the same geographical area studied via more conventional approaches. Stark and Williams (1995) examined the manganese removal efficiencies of 35 natural wetlands receiving coal mine drainage in Pennsylvania and West Virginia based on influent and effluent water quality data. Among this set of wetlands, they found that manganese treatment efficiency tended to be positively correlated with those wetlands that were larger in size, lacked channelized flow patterns, received an inflow of near neutral pH water low in dissolved iron, and contained a diversity of vascular plants and bryophytes. Tarutis et al. (1992) observed a lack of manganese accumulation in the sediments of a Pennsylvania wetland receiving coal mine drainage and suggested that long-term metal retention probably depended on the conversion of oxidized mineral phases found at the sediment surface (e.g., MnO_2) to reduced compounds at depth (e.g., $MnCO_3$). They suggested that wetlands for mine drainage treatment should be designed to enhance bacterial sulfate reduction and accelerate the formation of reduced manganese mineral species. Their wetland sediments showed little evidence of sulfate reduction, presumably a function of the lack of readily decomposable organic matter.

The apparent seasonal instability of MnO_2 in the surface sediments of our study wetland (Figure 10) suggests that manganese cycling in this wetland is similar to the pattern of periodic and spatial accumulation and remobilization observed elsewhere. Aguilar and Nealson (1998) observed that manganese was removed from the water column in Oneida Lake, New York, in the spring via conversion to particulate form and was deposited in the bottom sediments. During the summer months, reduced manganese moved from the sediments to the water column, where it increased in concentration during periods of stratification. Their data suggested an active internal manganese cycle within the lake, with a small net accumulation each year occurring in nodules located in the oxic portions of the lake.

Likewise, Bryant et al. (1997) noted higher inventories of manganese in sediment during the summer in an eutrophic Scottish lake compared to concentrations found in the fall and winter. They believed that periodic seasonal manganese accumulation was due to the higher pH and dissolved oxygen concentrations associated with a summer algal bloom. Epping et al. (1998) also found that benthic oxygenic photosynthesis in intertidal sediments strongly influenced sediment oxygen and pH microprofiles, suggesting that chemical precipitation

and reoxygenation dominated the retention of manganese in this environment. The formation of algal mats and subsequent MnO_2 precipitation (Knauer et al. 1999) are likely to strongly influence the accumulation of manganese in our study wetland as well. The undersides of floating algal mats in this wetland were dark in color in midsummer and tested positively for the presence of manganese oxides (data not shown). The subsequent settling of this algal material to the sediment surface would be expected to produce reducing conditions at the sediment surface as the mat decomposed, releasing dissolved manganese in the process. Because the intent of the current study was to demonstrate the use of redox gel probes to assess metal compound stability in the field, rather than to rigorously explain the manganese cycle within the wetland, insufficient data are available to address this issue. However, the periodic analysis of compound stability in sediments using the gel probe approach could be used to support such a hypothetical model.

Manganese oxide stability in the sediments of the study wetland appeared to be positively correlated with the spatial or seasonal variables of higher water flow rate, lower temperature, and a shallower thickness of underlying sediment. Increased MnO_2 stability in the path of increased water flow may relate to the disruption of the diffusive sublayer of the benthic boundary layer, which can slow the diffusion of ions (and O_2) between the overlying water and sediment (Berner 1980). Increased turbulent mixing due to increased water flow would be expected to enhance the rate of reductive ion efflux from near surface sediments and the influx of oxygen into sediments. Likewise, both lower temperatures and shallower sediments would theoretically limit the total amount of microbial activity and the porewater concentrations of MnO_2 reductants that would likely result.

Both $MnCO_3$ and MnS were selected as test compounds in this study because of their potential role as reduced manganese mineral species capable of being retained in sediments (Berner 1981). $MnCO_3$, in particular, has been suggested as the probable sink for dissolved Mn in deeper sediments, as porewater alkalinity increases and the $MnCO_3$ equilibrium is exceeded (Tarutis et al. 1992; van Cappellen et al. 1998). The calculated supersaturation of porewater with respect to rhodochrosite (Figure 5), and the apparent stability of solid $MnCO_3$ in gel probes (Figure 6) at or near the sediment surface in the study wetland, supports the hypothesis that this compound would tend to be stable with depth if formed. MnS is less likely to be an important solid phase in reduced sediments because of its extreme solubility, and the rather excessive sulfide concentrations required for its precipitation (Berner 1981). Both of these reduced manganese compounds frequently responded in a way opposite to that observed for MnO_2, remaining stable/solid at depths below which MnO_2 was no longer stable (Figure 7, site A and B). On other occasions, the behavior of these two compounds was seemingly independent of the stability of MnO_2 (Figure 7, sites C and D). We attribute these latter responses to probable localized differences in the suite of available "titrants" to which each compound will respond and the kinetics of those dissolution reactions. For example, $MnCO_3$ may be oxidized by dissolved oxygen in the uppermost sediment, yet possibly be unstable to much greater depths due to the presence of specific organic acids.

MnS was consistently less stable closer to the sediment-water interface than was FeS, although its stability at depth in these sediments suggests that geochemical conditions exist that would allow it to persist if formed. Gonzalez (1996) showed that lab sediments containing MnS were much more oxidized in the uppermost layers than the corresponding FeS sediments. Our attempts to identify MnS as a natural precipitate in these sediments were unsuccessful (data not shown). We believe that the probable scavenging effect of sulfide by interstitial iron would prevent the accumulation of sulfide concentrations high enough to precipitate MnS (Tarutis and Unz 1995). However, the potential for the formation and persistence of alabandite within sediment microniches where bacterial sulfate reduction is especially high remains a geochemical possibility (Davison 1993; Brendel and Luther 1995).

The spatial variability in stability demonstrated by both MnS and FeS gels suggests that these compounds may be useful indicators in determining the seasonal and areal variability of acid volatile sulfide (AVS) concentrations in sediments (Howard and Evans 1993). The ratio of molar concentrations of AVS and simultaneously extracted metals is often used to evaluate potential heavy metal toxicity in sediments, and the seasonal and spatial variation of the AVS pool is known to influence sediment toxicity (Leonard et al. 1993; Oehm et al. 1997).

Estimates of potential MnO_2 reduction rates were calculated for the wetland sediments using redox gel probe data. The loss of total manganese (initially present as MnO_2) over time in gel sections located at depths corresponding to the transitional zone between oxidized and reduced sediments (ca. -1 to -3 cm; Figure 8) was determined. This avoided an underestimation of reduction rates at lower depths due to a lack of reactive MnO_2 substrate. Manganese oxide reduction rate estimates at these depths were ca. 1.04×10^{-9} mol/L/s. These are similar to manganese oxide reduction rates of ca. 1.15 to 1.37×10^{-9} mol/L/s, determined for an anaerobic enrichment culture of marine sediment bacteria in laboratory experiments (Burdige et al. 1992). Similar rates have been reported for lab experiments examining the reduction of manganese oxides in the presence of sulfide (ca. 1.2×10^{-9} mol/L/s; DeVitre et al. 1988) and pyruvate (ca. 10^{-10} mol/L/s; Stone 1987). Reduction rates of ca. 10^{-11} to 10^{-12} mol/L/s were calculated by Davison (1993) for manganese oxides settling from oxic waters into an anoxic lake basin, based on the differences in manganese oxide concentrations in the particulates collected in sediment traps at different depths (Davison et al. 1982). This is consistent with observations that manganese oxides precipitated from natural waters were chemically more inert than synthetically prepared MnO_2 (DeVitre et al. 1988), and that several different manganese mineral phases may typically be present, each having different chemical reactivity to various reductants in sediment porewaters (Burdige and Nealson 1986).

In the present study, MnO_2 was solubilized in all sections of the gels during the in situ incubation period, even those within the overlying water (Figure 8). The minimum rate of MnO_2 reduction detected just below the sediment-water interface (Figure 8) was ca. 5.2×10^{-10} mol/L/s. It was common to observe the complete dissolution of immobilized MnO_2 in gel probes to extend above the sediment-water interface depending on the season and sampling location (data not shown). The extension of a MnO_2-reducing zone above the sediment-water interface is analogous to the occurrence of anoxic hypolimnia in lakes, and little solid manganese settling through the water column would be expected to be retained at depth unless it were within the lattice of allocthonous mineral precipitates (Davison 1993). The probable reductive role of dissolved ferrous iron on immobilized MnO_2 was also suggested by the apparent replacement of MnO_2 by iron at selected depth intervals in the sediment (Figure 9; Golden et al. 1988). The observed molar ratio of solubilized manganese to accumulated iron in the MnO_2 gel probes (Figures 8 and 9) typically remained below 2, consistent with the reaction (DeVitre et al. 1988):

$$2Fe^{2+} + MnO_2 + H_2O \rightarrow Fe_2O_3 + Mn^{2+} + 2H^+$$

This potential reductive reaction may be of more importance in these sediments when the periodic downward mixing of surface sediments occurs via bioturbation.

Conclusions

The redox gel probe method has been shown to be an inexpensive and relatively rapid diagnostic alternative to sediment coring and porewater analysis for the determination of metal

compound stability in shallow water sediments. In this article, the stabilities of particulate MnO_2, $MnCO_3$, MnS, and FeS were shown to be highly variable in time and space in the sediment of a wetland receiving circumneutral pH coal mine drainage. The immobilization of particulates in a gel matrix places some limitations on the interpretation of data, such as the potential direct role of bacteria in mineral dissolution. However, in situ reduction rate estimates for MnO_2 in gel probes closely approximated those calculated elsewhere based on laboratory and field data. The redox gel probe approach can also be envisioned as a diagnostic tool for the detection of environmental contaminants in porewaters, e.g., the replacement of iron in FeS by heavy metals, forming less soluble metal sulfides. Recently, immobilization of geochemically relevant bacteria in similar gel probes has been demonstrated (Edenborn and Brickett 2001). The general principles of these approaches should be applicable to a wide range of freshwater and marine sediments.

References

Aguilar C, Nealson KH. 1998. Biogeochemical cycling of manganese in Oneida Lake, New York. J Great Lakes Res 24:93–104.

Allison JD, Brown DS, Novo-Gradac KJ. 1991. MINTEQA2/PRODEFA2, a geochemical assessment model for environmental systems: Version 3.0 user's manual. Athens, GA: U.S. Environmental Protection Agency Report 1600/3-91/021.

Berner RA. 1980. Early diagenesis. Princeton, NJ: Princeton University Press, 241p.

Berner RA. 1981. A new geochemical classification of sedimentary environments. J Sediment Petrol 51:359–365.

Brandl H, Hanselmann KW. 1991. Evaluation and application of dialysis porewater samplers for microbiological studies at sediment-water interfaces. Aquat Sci 53:55–73.

Brendel PJ, Luther GW. 1995. Development of a gold amalgam voltammetric microelectrode for the determination of dissolved Fe, Mn, O_2, and S (-II) in porewaters of marine and freshwater sediments. Environ Sci Technol 29:751–761.

Bryant CL, Farmer JG, MacKenzie AB, Bailey-Watts AE, Kirika A. 1997. Manganese behavior in the sediments of diverse Scottish freshwater lochs. Limnol Oceanogr 42:918–929.

Burdige DJ, Dhakar SP, Nealson KH. 1992. Effects of manganese oxide mineralogy on microbial and chemical manganese reduction. Geomicrobiol J 10:27–48.

Burdige DJ, Nealson KH. 1986. Chemical and microbiological studies of sulfide-mediated manganese reduction. Geomicrobiol J 4:361–387.

C & K Coal Company. 1986. Anderson Run progress report for Pennsylvania Department of Environmental Resources, Harrisburg, PA.

Davison W. 1993. Iron and manganese in lakes. Earth Sci Rev 34:119–163.

Davison W, Woof C, Rigg E. 1982. The dynamics of iron and manganese in a seasonally anoxic lake; direct measurement of fluxes using sediment traps. Limnol Oceanogr 27:987–1003.

Davison W, Fones GR, Grime GW. 1997. Dissolved metals in surface sediment and a microbial mat at 100-μm resolution. Nature 387:885–888.

DeVitre RR, Buffle J, Perret D, Baudat R. 1988. A study of iron and manganese transformations at the O_2/S(-II) transition layer in an eutrophic lake (Lake Bret, Switzerland): A multimethod approach. Geochim Cosmochim Acta 52:1601–1613.

Edenborn HM, Brickett LA. 2001. Bacteria in gel probes: Comparison of the activity of immobilized sulfate-reducing bacteria with in situ sulfate reduction in a wetland sediment. J Microbiol Methods 46:51–62.

Edenborn HM, Brickett LA, Chaiken RF. 2002. Determination of trace element stability in sediments using redox gel probes: Probe construction and theoretical performance. Geomicrobiol J 19:465–483.

Epping EHG, Schoemann V, de Heij H. 1998. Manganese and iron oxidation during benthic oxygenic photosynthesis. Estuar Coastal Shelf Sci 47:753–767.

Flanagan NE, Mitsch WJ, Beach K. 1994. Predicting metal retention in a constructed mine drainage wetland. Ecol Eng 3:135–159.

Golden DC, Chen CC, Dixon JB, Tokashiki Y. 1988. Pseudomorphic replacement of manganese oxides by iron oxide minerals. Geodermatology 42:199–211.

Gonzalez AM. 1996. A laboratory-formulated sediment incorporating synthetic acid-volatile sulfide. Environ Sci Technol 15:2209–2220.

Harper MP, Davison W, Tych W. 1997. Temporal, spatial, and resolution constraints for in situ sampling devices using diffusional equilibration: Dialysis and DET. Environ Sci Technol 31:3110–3119.

Hesslein RH. 1976. An in-situ sampler for close interval porewater studies. Limnol Oceanogr 21:912–914.

Howard DE, Evans RD. 1993. Acid-volatile sulfide (AVS) in a seasonally anoxic mesotrophic lake: Seasonal and spatial changes in sediment AVS. Environ Toxicol Chem 12:1051–1057.

Hunt RJ, Krabbenhoft DP, Anderson MP. 1997. Assessing hydrogeochemical heterogeneity in natural and constructed wetlands. Biogeochemistry 39:271–293.

Hyman DM, Watzlaf GR. 1997. Metals and other components of coal mine drainage as related to aquatic life standards. Proceedings of the 14th annual National Meeting of the American Society of Surface Mining and Reclamation, Austin, TX. p 531–545.

Knauer K, Jabusch T, Sigg L. 1999. Manganese uptake and Mn (II) oxidation by the alga Scenedesmus subspicatus. Aquat Sci 61:44–58.

Krom MD, Davison P, Zhang H, Davison W. 1994. High resolution pore water sampling using a gel sampler: An innovative technique. Limnol Oceanogr 39:1967–1972.

Leonard EN, Mattson VR, Benoit DA, Hoke RA, Ankley GT. 1993. Seasonal variation of acid volatile sulfide concentration in sediment cores from three northeastern Minnesota lakes. Hydrobiologia 271:87–95.

Morton RA, White WA. 1997. Characteristics of and corrections for core shortening in unconsolidated sediments. J Coastal Res 13:761–769.

Oehm NJ, Luben TJ, Ostrofsky ML. 1997. Spatial distribution of acid-volatile sulfur in the sediments of Canadohta Lake, PA. Hydrobiologia 345:79–85.

Shuttleworth SM, Davison W, Hamilton-Taylor J. 1999. Two-dimensional and fine structure in the concentrations of iron and manganese in sediment porewaters. Environ Sci Technol 33:4169–4175.

Stark LR, Wenerick WR, Williams FM, Wuest PJ. 1995. The effects of pH, flow rate, and carbon supplementation on manganese retention in mesocosm wetlands. J Environ Qual 24:816–826.

Stark LR, Williams FM. 1995. Assessing the performance indices and parameters of treatment wetlands for H^+, Fe, and Mn retention. Ecol Eng 5:433–444.

Stone AT. 1987. Microbial metabolites and the reductive dissolution of manganese oxides: Oxalate and pyruvate. Geochim Cosmochim Acta 51:919–925.

Tarutis WJ, Unz RF. 1990. Chemical diagenesis of iron and manganese in constructed wetlands receiving acidic mine drainage. In: Cooper PF, Findlater BC, eds. Constructed wetlands in water pollution control. Proceedings of the International Conference on the Use of Constructed Wetlands in Water Pollution Control, Cambridge, UK. Oxford: Pergamon Press, p. 429–440.

Tarutis WJ, Unz RF. 1995. Iron and manganese release in coal mine drainage wetland microcosms. Wat Sci Tech 32:187–192.

Tarutis WJ, Unz RF, Brooks RP. 1992. Behavior of sedimentary Fe and Mn in a natural wetland receiving acidic mine drainage, Pennsylvania, U.S.A. Appl Geochem 7:77–85.

U.S. Environmental Protection Agency. 1983. Methods for chemical analysis of water and wastes. EPA/600/4-79/020, Cincinnati, OH.

van Cappellen P, Viollier E, Roychoudhury A, Clark L, Ingall E, Lowe K, Dichristina T. 1998. Biogeochemical cycles of manganese and iron at the oxic-anoxic transition of a stratified marine basin (Orca Basin, Gulf of Mexico). Environ Sci Technol 32:2931–2939.

Wahl KL, Thomas WO, Hirsch RM. 1995. Stream-gaging program of the U.S. Geological Survey. Reston, VA: U.S. Geological Survey Circular 1123. 22 p.

Weiser HB, Milligan WO. 1931. The transformation from rose to green manganous sulfide. J Phys Chem 35:2330–2344.